ELSEVIER

Chemical Engineering Journal 131 (2007) 273–281

Chemical Engineering Journal

www.elsevier.com/locate/cej

Experimental and analytical investigations of airlift pumps operating in three-phase flow

S.Z. Kassab [a], H.A. Kandil [a], H.A. Warda [a], W.H. Ahmed [b,*]

[a] *Mechanical Engineering Department, Faculty of Engineering, Alexandria University, Alexandria, Egypt*
[b] *Component Life Technology, Atomic Energy of Canada Ltd., Chalk River Laboratories, Ontario, Canada*

Received 2 September 2005; received in revised form 2 November 2006; accepted 7 December 2006

Abstract

Based on the control volume approach, a theoretical model is developed to predict the airlift-pump performance in air–water–solid three-phase flow. Experiments were performed using coarse, irregular non-uniform crushed pink limestone particles. The effect of the submergence ratio and size of solid particles on the pump performance are investigated. The predictions of the proposed model are in good agreement with the experimental results of an airlift pump conveying solid particles. In addition, the comparison with the experimental results shows that the proposed model can be used, with good accuracy, to predict the performance of airlift pumps operating in air–water two-phase flow when the solid mass flow rate is set to zero.

Keywords: Airlift pump; Three-phase flow; Multi-phase flow in a vertical pipe; Solid transport

1. Introduction

The principles of airlift pumping were understood since about 1882, but practical use of airlift did not appear until around the beginning of the twentieth century. In comparison with other pumps, the particular merit of the airlift pump is the mechanical simplicity. Moreover, airlift pumps have several advantages over other pumps. They do not have any moving parts, no lubrication or wear problems. Thus, theoretically, the maintenance of this kind of pumps has a lower cost and higher reliability. Airlift pumps can be used for lifting corrosive and/or toxic substances in chemical industries, conveying slurries in mining, lifting manganese nodules from deep-sea bed at about 4000–6000 m [1], sludge removal in sewage treatment plants [2], operating continuous sand filters, and lifting life fish in airlift fish pumps. Moreover, they are easy to use in irregularly shaped wells where other deep well pumps do not fit. Airlift pumps are not available from suppliers, but they are very simple to build. Generally, airlift pumping is most efficient when the static liquid level is high. The main disadvantages of airlift pumps are their low efficiencies and requirement of a very large submergence to obtain high efficiency as compared to other pumps.

Many studies were performed to investigate the performance of airlift pumps operating in two-phase flow [3–5]. For airlift pumps conveying solid particles, several experimental studies were reported in the literature, however, only few studies were carried out to analyze their performance theoretically. Moreover, only uniform solid particles were used to investigate the pump performance.

An early study of airlift pumps lifting solids was performed by Kato et al. [6] for a low-head airlift pump used to lift uniform solid particles. They analyzed the pump based on an existing theory of two-phase flow. The model was developed by coupling the momentum equation of two-phase flow and the equation of motion of a single solid particle. The performance of a typical airlift pump was computed and its fundamental characteristics were obtained with neglecting the compressibility of air. They validated their model by comparing its results with the results obtained using a 19 mm diameter pipe as a riser and small glass balls (density = 2600 kg/m^3) of 3.75 and 7.57 mm diameters as test solid particles.

Kato et al. [7] extended the study of Kato et al. [6] for high-head airlift pumps where the compressibility of air was taken into consideration. The test particles used in the experiments were

* Corresponding author. Tel.: +1 905 529 0373; fax: +1 905 572 7944.
E-mail address: ahmedw@aecl.ca (W.H. Ahmed).

1385-8947/$ – see front matter © 2006 Elsevier B.V. All rights reserved.
doi:10.1016/j.cej.2006.12.009

Nomenclature

A	pipe cross sectional area (m^2)
c	distribution coefficient
D	pipe diameter (m)
f	coefficient of friction
g	gravitational acceleration (m/s^2)
h_d	static lift
H_s	static head (m)
J	volumetric flux (m/s)
K	friction factor
L	length along the pipe (m)
L_2	suction part (two-phase flow) (m)
L_3	delivery part (three-phase flow) (m)
m	flux of three-phase mixture
P	pressure (N/m^2)
Q	volume flow rate (m^3/s)
Re	Reynolds number
S	slip ratio
S_r	submergence ratio
u	velocity (m/s)
x	quality

Greek letters

ε	void fraction (volumetric fraction)
ρ	density (kg/m^3)
τ	shear stress (N/m^2)

Subscripts

f	friction
G	gas
L	liquid
LS	liquid–solid
S	solid
3	three-phase flow

glass balls of 50 mm diameter. They concluded that, the flow of high-head airlift pumps for solid particles could be analyzed by extending the analysis of the low-head case study.

Yoshinaga and Sato [8] questioned the validity of the momentum balance method and the empirical correlations used by previous investigators because they were not universally confirmed. Moreover, the multi-fluid model is not satisfactory applicable because several constitutive equations for three-phase flow are not sufficient to model the performance of airlift pumps lifting solids. As a result, none of the models, together with their relating constitutive equations, have been sufficiently successful to be used in engineering applications. They developed a theoretical model based on the momentum equation combined with some empirical correlations from pervious studies of three-phase flow. They studied also the effects of pipe diameter, the submergence ratio, and the size and density of the solid balls on the pump performance. In their experimental work, they used ceramic spheres of diameters of 6.1 and 9.9 mm (density = 3630 kg/m^3). Two pipes of 26 and 40 mm diameters were used with the uniform ceramic balls. Several combinations of the ceramic balls were lifted using the 40 mm diameter pipe. Submergence ratios of 0.6, 0.7, and 0.8 were tested. The theoretical model was validated by comparison with the experimental results.

Gas–liquid–solid three-phase flow in an airlift pump was also modeled by Margaris and Papanikas [9] by a system of differential equations driven from the fundamental conservation equations of continuity and momentum. Their approach led to a more general mathematical model that is applicable to a wide range of installations, from small airlift pump to very large systems. The analysis is based on a separated flow model. The set of equations were programmed in a computer code, which they used as a tool for optimizing the design of airlift pump installations. They concluded that their model is capable of obtaining the important parameters such as drag coefficients of both solid and liquid; pump efficiency, and optimum values of pipe diameter, length, and injection point.

Another theoretical analysis of the three-phase flow in a vertical pipe was presented by Hatta et al. [1]. The system of governing equations used is based on the one-dimensional multi-fluid model. The transitions of gas flow patterns are taken into account in the system of governing equations. The analysis was later extended to include the effects of the air compressibility Hatta et al. [10], where a sudden change of the pipe diameter was introduced to account for the compressibility of air. They found that the motion of the solid particles depends strongly on the volumetric flux of the gas-phase as well as the submergence ratio.

In the present work, a theoretical model is developed to predict the airlift pump performance when operating in three-phase flow regime. The capability of the model in predicting the performance of the airlift pump lifting coarse irregular particles is examined by comparing its results with the experimental results of Ahmed [11].

It is known that airlift pump is not a fluid transport installation but it is only a fluid transfer device essentially short. Therefore, in practice, there is no need to know the pipe losses in an airlift pump installation. As a pumping device, however, the airlift pump has a large variation in efficiency, and any reduction of flow below its optimum range increases hydraulic losses, irrespective of a lower pipe friction loss. For this reason a familiarity with the hydraulic performance of the airlift pump is much more important than the knowledge of the pipe friction loss. Therefore, the present work is concentrated on studying the parameters affecting the design of airlift installations. These parameters are:

- The ratio between the submergence (static lift) and the total length of the pipe (the sum of the static head and static lift), which is known as the submergence ratio, S_r. The submergence ratio is the most important factor in the pump design.
- Volume flow rate of the fluid (pump capacity), Q.
- Static lift, h_d, which is the height to which water or solid–water mixture is to be raised.
- The important solid characteristics, such as the particle size.

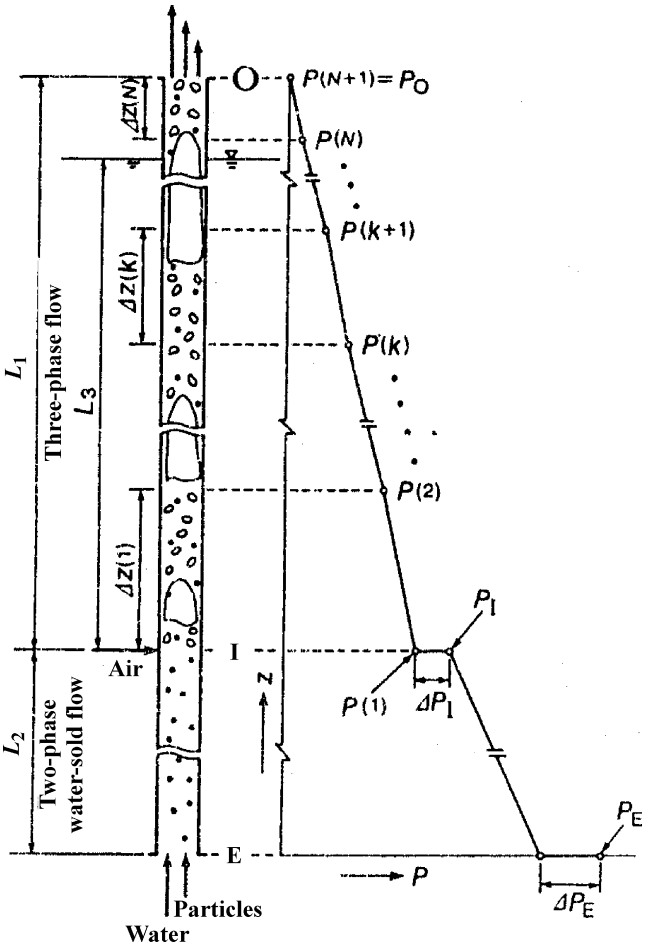

Fig. 1. Diagram of the airlift pump and the axial pressure distribution [8].

2. Theoretical analysis

There have been numerous publications suggesting procedures for the design and the satisfactory operation of an airlift pump lifting coarse particles. As listed by Yoshinaga and Sato [8], theoretical studies have been presented for uniform particles by Kato et al. [6,7], Kawashima et al. [12], Usami and Saito [13], Dedegil [14] and Tomiyama et al. [15]. None of the above models, together with their related constitutive equations, have been sufficiently successful yet to be used in engineering applications. Some of these studies are based on momentum balance (e.g. [6,7,13]), empirical correlations (e.g. [12]), power balance [14] and a multi-fluid model [15].

In the present study, a general analysis method for three-phase flow and a design model for an airlift pump that was proposed by Yoshinaga and Sato [8], is modified based on the present experimental installation [16].

The airlift pump with a vertical pipe having uniform cross-sectional area, which is used in the analysis, is illustrated in Fig. 1 [8] together with the diagram of the pressure distribution, P, in the flow direction, z. The pump consists of two parts: a suction pipe in which a two-phase water–solid mixture flows and an up-riser in which a three-phase air–water–solid mixture flows. The symbols E, I and O denote the cross sections of the suction pipe inlet, the air injector and the up-riser outlet, respectively.

The momentum equation is applied to a control volume bounded by the pipe wall and the cross sections E and O. Assuming the solid particles to be conveyed are, in general, having same size and density. The momentum equation may therefore be written as

$$A\{J_{\mathrm{L}}\rho_{\mathrm{L}}u_{\mathrm{L,E}} + J_{\mathrm{S}}\rho_{\mathrm{S}}u_{\mathrm{S,E}}\} - A\{J_{\mathrm{G,O}}\rho_{\mathrm{G,O}}u_{\mathrm{G,O}} + J_{\mathrm{L}}\rho_{\mathrm{L}}u_{\mathrm{L,O}} + J_{\mathrm{S}}\rho_{\mathrm{S}}u_{\mathrm{S,O}}\} - \pi D\int_E^I \tau_{\mathrm{LS}}\,\mathrm{d}z - \pi D\int_I^O \tau_3 - A\int_E^I \{\rho_{\mathrm{L}}\varepsilon_{\mathrm{L,LS}} + \rho_{\mathrm{S}}\varepsilon_{\mathrm{S,LS}}\}g\,\mathrm{d}z - A\int_I^O \{\rho_{\mathrm{G}}\varepsilon_{\mathrm{G}} + \rho_{\mathrm{L}}\varepsilon_{\mathrm{L,3}} + \rho_{\mathrm{S}}\varepsilon_{\mathrm{S,3}}\}g\,\mathrm{d}z + A\int_I^O \{\rho_{\mathrm{L}}g(L_2+L_3)\} = 0 \quad (1)$$

where J is the volumetric flux, u the velocity, ε the volumetric fraction, ρ the density, τ the shear stress, and g is the gravitational acceleration. The subscripts G, L, S, LS and 3 represent air, water, solid, two-phase water–solid mixture and three-phase air–water–solid mixture, respectively. The subscripts E, I and O represent the cross sections of the inlet, air injector and the outlet, respectively. The first and second terms of Eq. (1) denote the momentum which enters through E and leaves through O. The third and fourth terms denote the frictional pressure loss in the two-phase water–solid flow and in the three-phase flow. The fifth and sixth terms denote the weight of the two-phase water–solid mixture and that of the three-phase mixture. The seventh term denotes the pressure force of the surrounding water acting on E. The pressure at O is assumed to be equal to atmospheric pressure. The third term on the left-hand side of Eq. (1), as a result, is rewritten as

$$\pi D\int_E^I \tau_{\mathrm{LS}}\,\mathrm{d}z = A\left\{\frac{\Delta P_{\mathrm{f,LS}}}{\Delta z}L_2 + \Delta P_{\mathrm{E}}\right\} \quad (2)$$

where $\Delta P_{\mathrm{f,LS}}/\Delta z$ is the frictional pressure gradient in two-phase water solid flow and ΔP_{E} is the entrance pressure drop of the suction pipe, which is the sum of the entrance fitting loss and entrance length loss occurs at E.

Also, the sixth term in Eq. (1) is written as

$$A\int_E^I \{\rho_{\mathrm{L}}\varepsilon_{\mathrm{L,LS}} + \rho_{\mathrm{S}}\varepsilon_{\mathrm{S,LS}}\}g\,\mathrm{d}z = A\{\rho_{\mathrm{L}}\varepsilon_{\mathrm{L,LS}} + \rho_{\mathrm{S}}\varepsilon_{\mathrm{S,LS}}\}gL_2 \quad (3)$$

The up-riser is divided into N nodes in the flow direction because the frictional pressure gradient in the three-phase flow cannot be estimated at the middle of I and O due to the expansion of air. The distance between each two nodes is assumed to be the same.

Let $P(k)$ and $P(k+1)$ be the absolute pressures of the inlet and the outlet at kth node, the fourth term on the left-hand side of Eq. (1) is, as a result, rewritten as

$$\pi D\int_I^O \tau_3\,\mathrm{d}z = A\left\{\sum_{k=1}^{N}\frac{\Delta P_{\mathrm{f},3}(k)}{\Delta z(k)}\Delta z + \Delta P_{\mathrm{I}}\right\} \quad (4)$$

where $\Delta P_{f,3}/\Delta z$ is the frictional pressure gradient in the three-phase flow at the kth node.

The gravity force at each node is estimated at the middle of each element, then the sixth term in (1) becomes

$$A\int_I^O \{\rho_G\varepsilon_G + \rho_L\varepsilon_{L,3} + \rho_S\varepsilon_{S,3}\}g\,dz = A\sum_k^N [\{\rho_G(k)\varepsilon_G(k) + \rho_L\varepsilon_{L,3}(k) + \rho_S\varepsilon_{S,3}(k)\}g\Delta z] \quad (5)$$

The correlations of volumetric fractions and pressure drops in Eqs. (1)–(5) are obtained from the following correlations.

The volumetric fraction of particles in a three-phase flow is expressed by

$$\varepsilon_{S,3} = \frac{J_S}{u_S} \quad (6)$$

where J_S is the volumetric flux of solid particles and u_S is the velocity of particles in a three-phase flow.

Based on the correlations for the velocity of particles in a three-phase flow proposed by Sato et al. [17], u_S is expressed by

$$u_S = c\frac{m}{\rho_A} + u_{SW} \quad (7)$$

where c is the distribution coefficient, m the flux of the three-phase mixture, ρ_A the apparent density of the three-phase mixture and u_{SW} is the wall-affected settling velocity of the particles in an imaginary still three-phase mixture with ρ_A. Where,

$$c = 1 + c_1 \exp\left\{-5\frac{\varepsilon_{S,3}}{1-\varepsilon_G}\right\}, \quad (8)$$

$$m = \rho_G J_G + \rho_L J_L + \rho_S J_S, \quad (9)$$

$$\rho_A = \left(\frac{\rho_3}{\rho_{LS,3}}\right)^{1.5}\rho_{LS,3} \quad (10)$$

$$u_{SW} = \left[1 - \left\{\frac{d_S}{D}\right\}^2\right]\left\{1 - \frac{\varepsilon_{S,3}}{1-\varepsilon_G}\right\}^{2.4}\sqrt{\frac{(\rho_L/\rho_A)S - 1}{S-1}}u_{ST} \quad (11)$$

The factor c_1 in Eq. (8) is about 0.2 for a spherical particle. Sato et al. [17] proposed Eq. (10) by treating a three-phase flow as a two-phase air-slurry flow. In (10), ρ_3 is the mean density of the three-phase mixture and $\rho_{LS,3}$ is the mean density of the slurry.

The above parameters are expressed by

$$\rho_3 = \rho_G\varepsilon_G + \rho_L\varepsilon_{L,3} + \rho_S\varepsilon_{S,3} \quad (12)$$

$$\rho_{LS,3} = \rho_L\frac{\varepsilon_{L,3}}{1-\varepsilon_G} + \rho_S\frac{\varepsilon_{S,3}}{1-\varepsilon_G} \quad (13)$$

where S is the specific density of the particles and u_{ST} is the free settling velocity of a single particle in still water.

The volumetric fraction of particles in two-phase water–solid flow, from section E to I, is obtained from (6) by setting J_G and ε_G in (8), (9) and (11)–(13) equal to zero. The volumetric fraction of air in a three-phase flow was proposed by Sato et al. [17] as

$$\varepsilon_G = \left[1 + 0.4\frac{\rho_G}{\rho_{LS,3}}\left(\frac{1}{x} - 1\right) + 0.6\frac{\rho_G}{\rho_{LS,3}}\left(\frac{1}{x} - 1\right) \times \left\{\frac{(\rho_{LS,3}/\rho_G) + 0.4((1/x) - 1)}{1 + 0.4((1/x) - 1)}\right\}^{0.5}\right]^{-1} \quad (14)$$

where x is defined as the quality and given by $x = \rho_G J_G/m$.

If the volumetric fractions of gas and solid are obtained, the volumetric fraction of water is then given by

$$\varepsilon_{L,3} = 1 - \varepsilon_G - \varepsilon_{S,3} \quad (15)$$

Frictional pressure drop in the water–solid two-phase flow is obtained from the correlation as mentioned by Yoshinaga and Sato [8].

$$\frac{\Delta P_{f,LS}}{\Delta z} = \lambda_{LS}\frac{1}{D}\frac{\rho_{LS}}{2}\{J_L + J_S\}^2 \quad (16)$$

where the friction factor is given by

$$\lambda_{LS} = 0.316 Re_{LS}^{-0.25} \quad (17)$$

The Reynolds number is expressed by

$$Re_{LS} = \frac{\{J_L + J_S\}D}{\nu_L} \quad (18)$$

The entrance pressure drop in the two-phase water–solid, ΔP_E is calculated from Dedegil Dedegil's equation [14] which correlates the entrance pressure drop in a suspension flow containing fine particles, by treating the suspension as a two-phase water–coarse particles mixture, the equation can be written as follows:

$$\Delta P_E = (\xi + \xi_E)\frac{\rho_{LS}}{2}\{J_L + J_S\}^2 \quad (19)$$

In the present study, the coefficient of inlet fitting loss, ζ, was set equal to 1.56, and the coefficient of the entrance length loss, ζ_E, was set equal to 2.5. These factors were determined experimentally for a pipe with sharp entrance.

The entrance loss in three-phase flow is calculated as a pressure drop at section I using Dedegil Dedegil's equation [14], as follows:

$$\Delta P_l = \xi_1\left[\frac{\rho_{LS,3}}{2}\left\{\frac{J_L + J_S}{1-\varepsilon_G}\right\}^2 - \frac{\rho_{LS}}{2}\{J_L + J_S\}^2\right] \quad (20)$$

ζ_1 was set equal to 1.5 in the present calculations.

In the original model presented by Yoshinaga and Sato [8] two variables are used as the input values, namely volumetric flux of solid (J_S) and volumetric flux of gas (J_G). While the output of the model is the volumetric flux of liquid (J_L), which is not a good representation of the real engineering case where the air flow rate is the only input parameter and the output is both the water and solid flow rates. In the modified model, developed in the present study, the equation obtained by Stenning and Martin [18] is used to obtain an initial relation between the water lifted and the input gas flow rate. This equation was previously investigated by the present authors in studying the performance of airlift pump

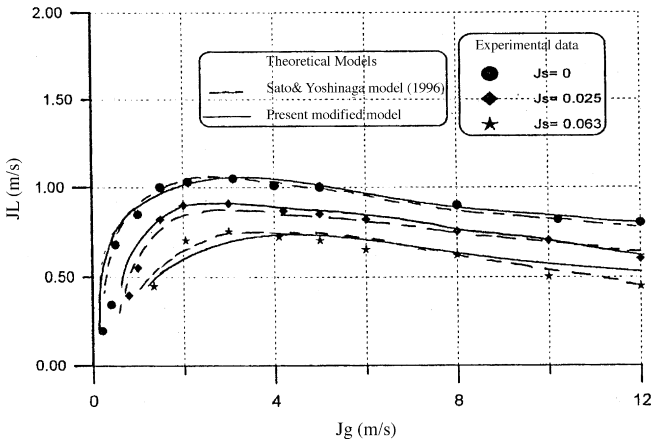

Fig. 2. Comparison between Yoshinaga and Sato [8] model and the present modified model.

lifting water only [19]. The model predicts the performance of the pump accurately for the two-phase flow. The results obtained by the model are used to estimate the water flow rate for each value of the input air mass flow rate. These results are used for estimating the water flow rate with solid particles as a first iteration. This assumption is quite good for the slug flow region because there is no sensible difference between the water flow rates for two-phase flow and three-phase flow [16].

The relation between the water and air flow rates was obtained by Stenning and Martin [18] in the form:

$$\frac{H_s}{L} - \frac{1}{1+(Q_G/sQ_L)} = \frac{V_l^2}{2gL}\left[(K+1)+(K+2)\frac{Q_G}{Q_L}\right] \quad (21)$$

where K is the friction factor and S is the slip factor. In the original model by Stenning and Martin, constant values were assumed for both K and s. Later the model was modified by Ahmed [11] where friction factor K is calculated from the following correlation.

$$K = \frac{4fL}{D} \quad (22)$$

where f is friction coefficient which is determined from the Colebrook–White equation for turbulent flow. The slip ratio, S, is determined from the expression proposed by Griffith and Wallis [20] in the following equation:

$$s = 1.2 + 0.2\frac{Q_G}{Q_L} + \frac{0.35\sqrt{gD}}{V_l} \quad (23)$$

3. Validation of the proposed model

Before validating the modified model in predicting the experimental data performed by Kassab et al. [16], the model is first used to predict the data presented by Yoshinaga and Sato [8] to show the effect of the proposed modifications and simplification on the original model as shown in Fig. 2.

Fig. 2 shows a comparison between the volumetric gas flux, J_G, and the volumetric liquid flux, J_L, from the experimental work of Yoshinaga and Sato [8], as well as the results obtained using their model, and the results predicted by the modified model proposed in the present study. The comparison is based on using spherical particles and a volumetric solid flux ($J_S \leq 0.063$ m/s). It is noted that, the modified model is in good agreement with the model proposed by Yoshinaga and Sato [8]. This means that the modified model can be used to predict the pump performance for non-uniform coarse solid particles with an acceptable accuracy.

It should be noted that there are some limitations on the usage of the model when the pump riser is very long as in the application in lifting manganese from deep sea-beds, where the compressibility of air is significant and can not be neglected [10].

In Fig. 2, the comparisons show that, good agreement between the present model and the experimental data obtained when the airlift pump operates in two-phase flow. This means that, the model could be used to investigate also, the performance of the airlift pump lifting liquid only by setting the volumetric flux of solids to zero.

4. Experimental setup

The experimental setup used in the present study is schematically shown in Fig. 3. It consists of a vertical transparent pipe (riser) (1), of 3.75 m length and 25.4-mm inner diameter, and a down-comer pipe (2) of 30 mm inner diameter. The riser pipe is divided into three sections to allow studying the effects of

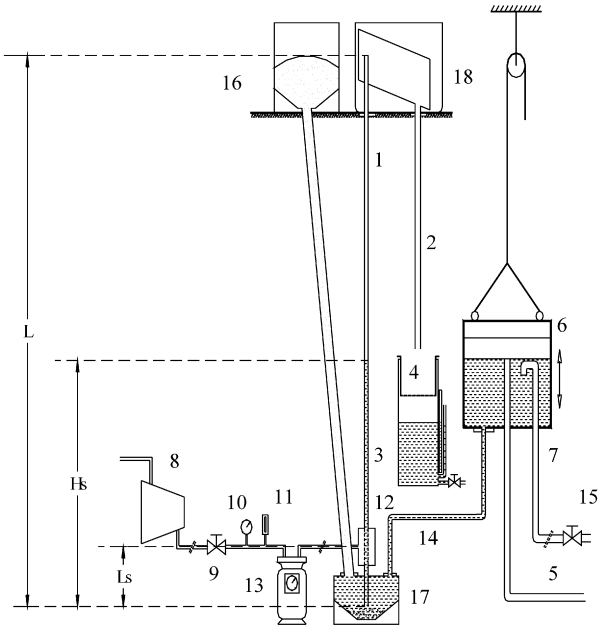

1. Riser
2. Down comer
3. Water collecting tank
4. Strainer
5. Drain
6. Water feeding tank
7. Over-flow pipe
8. Compressor
9. Regulator
10. Pressure gage
11. Thermometer
12. Air-jacket
13. Bellow meter
14. Feeding-water line
15. Control valve
16. Solid-particle tank
17. Mixing box
18. Delivery tank

Fig. 3. A schematic diagram of the airlift pump setup used for conveying solids. (1) Riser, (2) down comer, (3) water collecting tank, (4) strainer, (5) drain, (6) water feeding tank, (7) over-flow pipe, (8) compressor, (9) regulator, (10) pressure gage, (11) thermometer, (12) air-jacket, (13) bellow meter, (14) feeding-water line, (15) control valve, (16) solid-particle tank, (17) mixing box and (18) delivery tank.

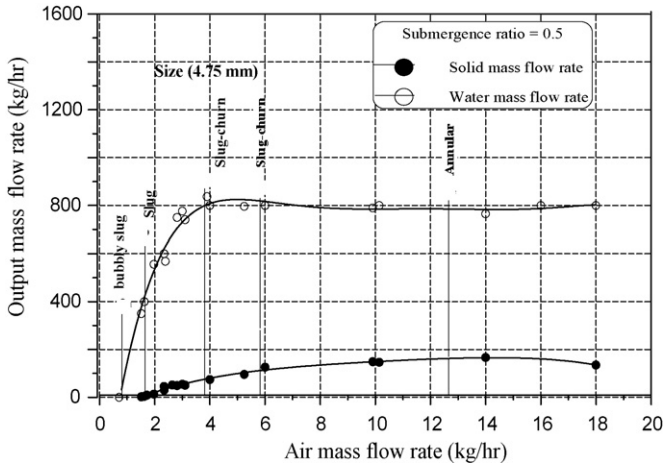

Fig. 4. Performance of airlift pump lifting solid particles at submergence ratio = 0.5.

changing the length. The upper end of the riser is connected to an overhead collecting tank where the air escapes to the atmosphere and water is collected in the tank. The water flow rate is measured by using the collecting tank (3). In order to separate the solid particles from the water–solid mixture a strainer (4) is used. A constant water head s kept in the movable water supply tank (6) is kept by overflowing the water through pipe (7). The water may be passed through a pipe (5) to the drain. The supply tank can also be moved up or down to change the submergence ratio. All pipes and tanks are made of transparent materials for clear visualization of the flow patterns.

Air is supplied to the air injection system from a central air compressor (8) through a 25-mm diameter pipeline to an on/off valve, then to a pressure-reducing valve (regulator) (9), where the pressure is reduced to the desired working pressure. Air is then injected into the riser at a constant pressure and can be measured by the pressure gage (10). A mercury thermometer (11) is used for measuring the upstream air temperature. A constant air mass flow rate passes through an air jacket (12) around the vertical pipe using the air injector. The volume of air is measured using a calibrated bellow-meter (13). The air injector consists of 56 small holes of 3 mm diameter uniformly distributed around the pipe perimeter in seven rows and eight columns to insure uniform feed of the air to the pipe at the mixing section 20 cm above the lower end of the pipe.

Table 1
Configuration of the strainers used to separate the particles in the present study

Size number	Average size (mm)
1	4.75
2	7.1
3	9.5
4	11.3

The solid tank (16) is used to feed the mixing box (17) with solid particles. The mixing box is designed to assure continuous presence of the solid particles at the pipe entrance.

Experiments were performed using irregular non-uniform coarse particles. The type of the solid particles used in the present study is crushed pink limestone with density of 2427 kg/m^3. The sizes of the solid particles are listed in Table 1. The mesh size of the strainers used for separating different particle sizes is used to define the particle size.

The performance of the airlift pump was investigated under various submergence ratios, namely 0.35, 0.5, 0.72 and 0.78. For each submergence ratio, and certain particle size, the airflow rate was varied and the corresponding mass flow rates of water and solids were measured. A specific operating procedure was followed for each run. The details of operating procedure as well as the uncertainty analysis are given by Ahmed [11].

5. Results and discussion

The variation of solid mass flow rate and water mass flow rate as a function of the air mass flow rate at submergence

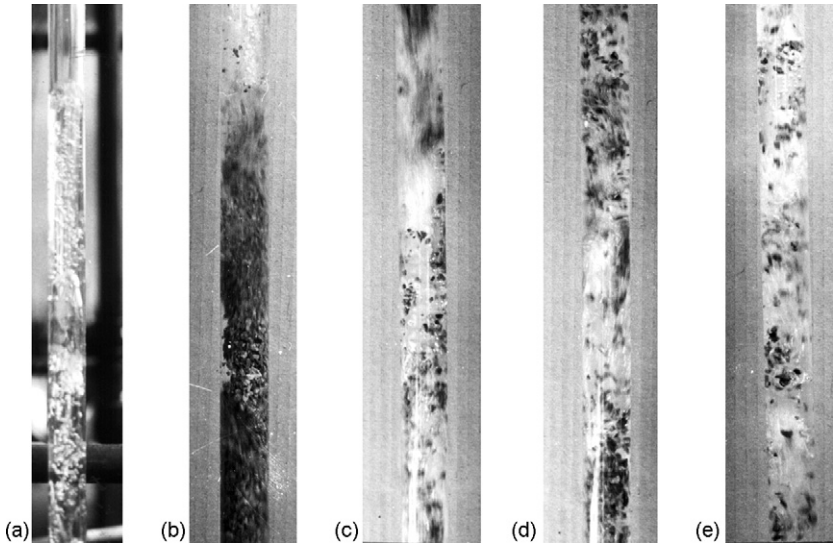

Fig. 5. Flow visualizations show the sequence of flow patterns at different values of air mass flow rate: (a) bubbly-slug; (b) slug; (c) slug-churn; (d) slug-churn; (e) annular.

ratio of 0.5, using particles of size 1, is shown in Fig. 4. With the aid of flow visualization performed during the experimental work, Fig. 5, it is noticed that, for low values of air flow rate, no water or solid are lifted as shown in Fig. 5a. This is because the buoyancy force is not enough to raise either water or solid.

When air mass flow rate increases, a small quantity of water is lifted without any solid particles. The flow pattern changes from bubbly to slug flow similar to the flow pattern in the case of airlift pump working in two-phase flow (air–water) presented by Kassab et al. [16].

When air flow rate increases slightly over 1.7 kg/h, flow of solid particles starts with a small value of 0.5 kg/h. Fig. 5b shows that the flow regime is totally slug. Solid particles are distributed uniformly in the water slugs. This is due to the higher friction drag between water and solid than that between air and solid. In addition, the particles in a gas slug are caught up with the chasing gas/liquid interface and then move in a liquid slug [21]. The same explanation was given by Kato et al. [6,7], who stated that, solid particles will fall much faster in air than in water because of a big difference in drag forces. The present study confirms the assumption that all solid particles are surrounded with water.

As the flow rate of air increases, the solid and water flow rates increase gradually until the water flow rate reaches a maximum value of 865 kg/h at air mass flow rate of 4 kg/h. The flow pattern at this point is mainly slug-churn flow, as can be seen in Fig. 5c and d.

As air flow rate increases further, the flow rate of water decreases by a small amount to 850 kg/h and approximately remains constant after this point while the flow pattern is completely annular flow. Meanwhile, the solid mass flow rate keeps in increasing to reach a maximum value of 175 kg/h where the air flow rate is about 12.7 kg/h, and the flow pattern, as can be seen from Fig. 5e, is annular flow. At this point the corresponding water mass flow rate is 800 kg/h. This slight decrease in the water flow rate is logic because more of the air energy was consumed to lift the solid particles instead of water.

The performance of airlift pump lifting solid particles of size 1, at different values of submergence ratio, is shown in Fig. 6. These results show that the performance of the airlift pump strongly depends on the submergence ratio. The relation between flow rate of solid particles and air flow rate has similar trend for all submergence ratios. At a constant value of air mass flow rate, as the submergence ratio increases the mass flow rate of the solid particles increases. Moreover, the starting point of lifting the solid particles moves to the left of the horizontal coordinate as the submergence ratio increases. This may be attributed to the increase of the static head available at the pump entrance, which helps the solid particles to flow earlier.

In the case of airlift pump conveying solid particles there is no definition of the efficiency in the literature. Therefore, in order to evaluate the performance of the airlift pump conveying solid particles, a new parameter called the effectiveness of the pump (E), is introduced as the ratio between the mass flow rate of the lifted solid particles and the mass flow rate of the injected air

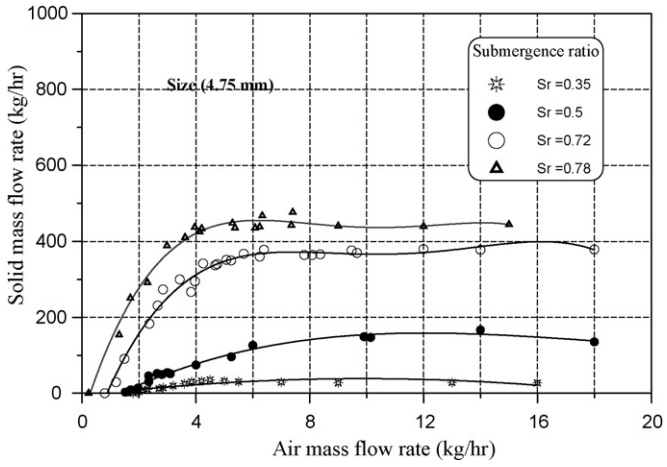

Fig. 6. Effect of submergence ratio on solid mass flow rate.

and can be written as

$$E = \frac{\dot{M}_{\text{solid}}}{\dot{M}_{\text{air}}} \tag{24}$$

Fig. 7 shows the relation between air mass flow rate and the effectiveness at submergence ratio of 0.5. The effectiveness increases rapidly with the increase of air mass flow rate up to 23, at air mass flow rate of 4 kg/h. As the airflow rate increases beyond this value, the effectiveness of the pump decreases. Comparing the results presented in Figs. 4 and 7, one can see that the maximum effectiveness does not exist at the point of maximum solid mass flow rate. Meanwhile, it is noted that the values of effectiveness of the airlift pumps are low. But this can be made up by the fact that no other pump can be used in the airlift pump applications such as recovery of underwater objects where the most important parameter is the safety of the objects.

The effectiveness of the airlift pump is also found to be strongly dependent on the submergence ratio. Fig. 8 shows that as the submergence ratio increases the effectiveness curves shift upward and the point of maximum effectiveness is located at smaller values of air mass flow rate. In addition, it is found that

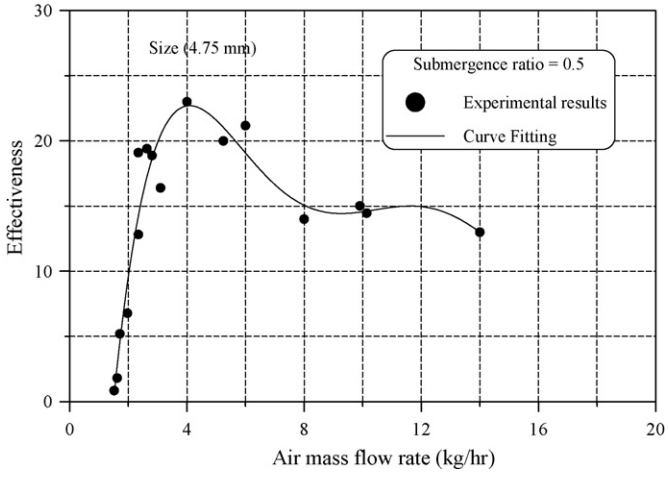

Fig. 7. Variation of pump effectiveness with air mass flow rate at submergence ratio = 0.5.

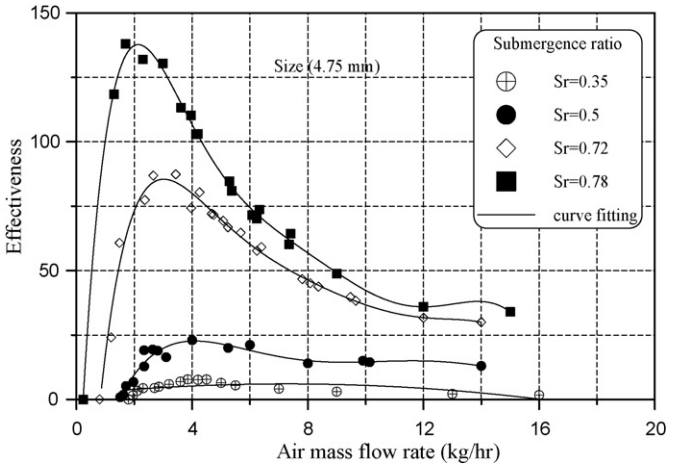

Fig. 8. Variation of pump effectiveness with air mass flow rate at different submergence ratios.

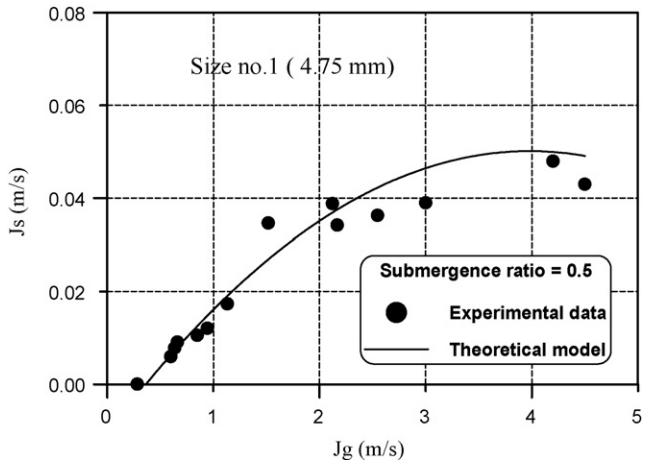

Fig. 10. Comparison between proposed model and the experimental results of Kassab et al. [16].

the maximum effectiveness has a maximum value of 143 at the highest value of submergence ratio used in the present study, i.e. 0.78.

For different particle sizes and at a submergence ratio of 0.72, Fig. 9 shows variation of air mass flow rate with the solid mass flow rate. The point where the solid flow starts is found to be different for each particle size. Further, it is noticed that, for the same air mass flow rate, as the size of solid particle increases the solid mass flow rate decreases. This is due to the deceleration of solid particle as the weight increases. Also, for small particles the surface area is greater than that for large ones for the same mass, therefore, the friction drag between solid and water in the case of larger sizes is lower than for smaller sizes. This results in a difficulty in carrying the large solid particles by liquid. Another explanation is given by Kato et al. [6,7] that the force required in lifting particles is much higher for large particles than for small ones. The present results agree with the results obtained by Kandil and Elmiligui [22] using an airlift pump to lift both course particles and sand.

6. Comparison between the proposed model and experimental results

In order to validate the present analysis, the results are compared with the experiments performed by the present authors [16]. This validation is presented in Figs. 10 and 11 through the comparison of predicted results, using the geometric parameters such as, pipe diameter of 25.4 mm and pipe length of 3.75 m, etc. The agreement between the proposed model and the experimental results is reasonable. There is a small deviation between the model results and the experimental results. This may be attributed to neglecting the interaction forces between the phases as pointed out by Hatta et al. [10], also neglecting the compressibility of air, and because the present analysis is based on empirical correlations.

The present model can be used to predict the airlift pump performance operating in two-phase flow by setting the value of the solid mass flux to zero. This is shown in Fig. 12, where the performance predicted by using the model for two-phase flow and the proposed model for the three-phase flow are plotted with the experimental data for a submergence ratio of 0.48 [19]. It

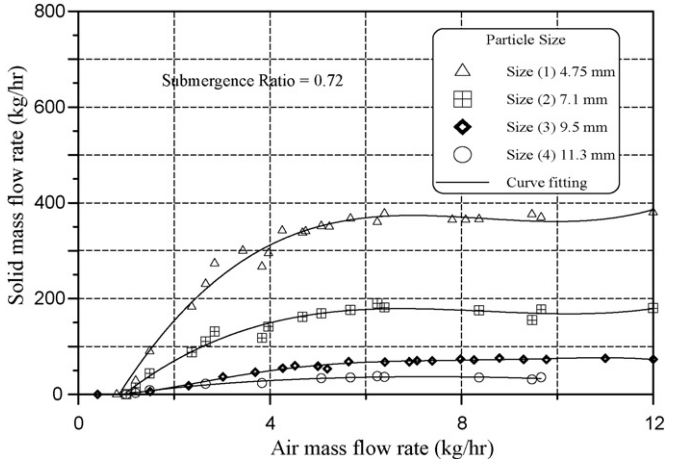

Fig. 9. Effect of particle size on the performance of airlift pump at submergence ratio = 0.72.

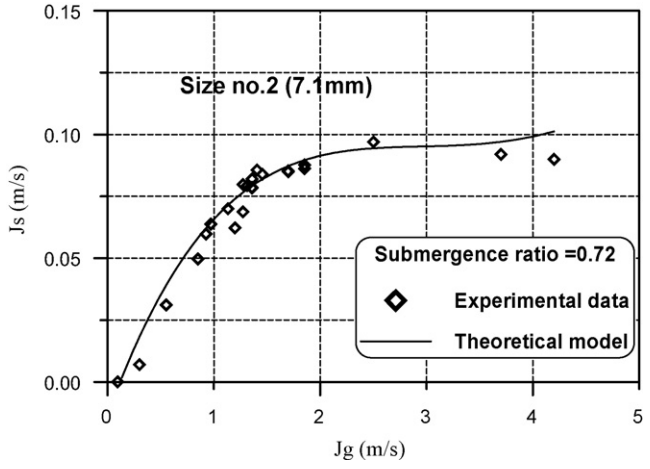

Fig. 11. Comparison between proposed model and the experimental results of Kassab et al. [16].

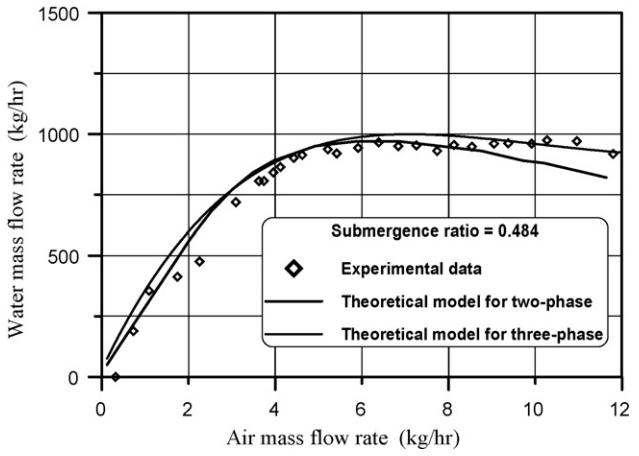

Fig. 12. Comparison between proposed models for two and three-phase flow regimes when the pump is lifting water.

is found that the present model for three-phase flow gives good agreement with the experimental results if adjusted to predict the two-phase flow.

7. Concluding remarks

The following concluding remarks can be obtained from the present work:

- The present modified model based on the original model proposed by Yoshinaga and Sato [8] for a uniform solid particle, gives a good agreement with experimental results for coarse particles that represent the more real engineering applications.
- The mass flow rate of the solid particles increases as the submergence ratio increases at the same airflow rate.
- The mass flow rate of the solid particles increases with the decrease of the particle size.
- The performance of the airlift pump, lifting water and solid particles, depends on the flow pattern in which the pump operates.
- The model proposed to predict the airlift pump performance operating in three-phase conditions, can be used to predict the performance of airlift pumps lifting liquid only by setting the value of the solid mass flow rate in the model to zero.
- The present model can be used in optimizing the design and operating conditions of airlift pumps operating in the three-phase flow. It can be used also to select the best geometric parameters for each application and operating conditions.

References

[1] N. Hatta, H. Fujimoto, M. Isobe, J. Kang, Theoretical analysis of flow characteristics of multiphase mixtures in a vertical pipe, Int. J. Multiphase Flow 24 (4) (1998) 539–561.

[2] B. Storch, Extraction of sludges by pneumatic pumping, in: Proceedings of the 2nd Symposium on Jet Pumps, Ejectors and Gas Lift Techniques, Churchill College, Cambridge, England, 1975, pp. G4-51–G4-60.

[3] D.J. Nicklen, The air lift pump theory and optimization, Trans. Inst. Chem. Engrs. 41 (1963) 29–39.

[4] N.N. Clark, R.J. Dabolt, A general design equation for air-lift pumps operating in slug flow, AIChE J. 32 (1986) 56–64.

[5] G.K. Awari, P.M. Ardhapurkar, D.G. Wakde, L.B. Bhuyar, Performance analysis of air-lift pump design, Proc.IMECH E Part C: J. Mech. Eng. Sci. 218 (2004) 1155–1161.

[6] H. Kato, S. Tamiya, T. Miyazawa, A study of an air-lift pump for solid particles and its application to marine engineering, JSME 18 (117) (1975) 286–294.

[7] H. Kato, S. Tamiya, T. Miyazawa, A study of an air-lift pump for solid particles and its application to marine engineering, in: Proceedings of the 2nd Symposium on Jet Pumps, Ejectors and Gas Lift Techniques, Churchill College, Cambridge, England, 1975, pp. G3-37–G3-49.

[8] T. Yoshinaga, Y. Sato, Performance of air -lift pump for conveying coarse particles, Int. J. Multiphase Flow 22 (2) (1996) 223–238.

[9] D.P. Margaris, D.G. Papanikas, A generalized gas–liquid–solid three-phase flow analysis for air-lift pump design, J. Fluids Eng. ASME 119 (1997) 995–1002.

[10] N. Hatta, M. Omodaka, F. Nakajima, T. Takatsu, H. Fujimoto, H. Takuda, Predictable model for characteristics of one-dimensional solid–gas–liquid three-phase mixtures flow along a vertical pipeline with an abrupt enlargement in diameter, Trans. ASME J. Fluids Eng. 121 (1999) 330–342.

[11] W.H. Ahmed, Performance of an AirLift Pump Operated in Multi-Phase Flow, M.Sc., Thesis, Alexandria University, Egypt.

[12] T. Kawashima, K. Noda, T. Masuyama, S. Oda, Hydrulic transport of soilds by air-lift pump, Nippon Kogyo Kaishi/J. Min. Metall. Inst. Jpn. 91 (1054) (1975) 765–772.

[13] T. Usami, T. Saito, Transport characteristics of solid particles carried by air-lift pump, Nippon Kogyo Kaishi 98 (1133) (1982) 597–602, 609.

[14] M.Y. Dedegil, Principles of Air-Lift Techniques, vol. 4, Encyclopedia Of Fluid Mechanics, Gulf, Houston, TX, 1987 (Chapter 12).

[15] A. Tomiyama, H. Minagawa, N. Furutani, T. Sakaguchi, Application of a two phase flow model based on local relative velocity to gas–liquid–solid three-phase flows, JSME Int. J. Ser. B 38 (4) (1995) 555–562.

[16] S.Z. Kassab, H.A. Kandil, H.A. Warda, W.H. Ahmed, Performance of an airlift pump operating in multiphase flow, in: Proceedings of the 12th International Mechanical Power Engineering Conference (IMPEC12), vol. 1, Mansoura, Egypt, October 30–November 1, 2001, pp. F1–F13.

[17] Y. Sato, T. Yoshinanga, M. Sadatomi, Data and empirical correlation for the mean velocity of coarse particles in a vertical three-phase air–water–solid particle flow, in: Proceedings of the International Conference Multiphase Flow, vol. 1, Tsukuba, Japan, 1991, pp. 363–366.

[18] A.H. Stenning, C.B. Martin, An analytical and experimental study of air-lift pump performance, Trans. ASME J. Eng. Power 90 (1968) 106–110.

[19] S.Z. Kassab, H.A. Kandil, H.A. Warda, W.H. Ahmed, Performance of an airlift pump operating in two-phase flow, in: Proceedings of the Seventh International Congress on Fluid Dynamics and Propulsion (ICFDP7), Cairo, Egypt, December 18–20, 2001.

[20] P. Griffith, G.B. Wallis, Two-phase slug flow, Trans. ASME J. Heat Transfer 83 (1961) 307–320.

[21] H. Natsuo, O. Masaaki, N. Fumitaka, F. Hitoshi, T. Hirohiko, Prediction of gas–liquid two-phase mixture flow in a vertical pipe with a sudden expansion in diameter, Steel Res. 71 (5) (2000) 153–160.

[22] H.A. Kandil, A.A. Elmiligui, Experimental study of an air lift pump lifting irregular solid particles, Alexandria Eng. J. 37 (1998) A35–A43.